6-29-2018

Simultaneous Regional Detection of Land-Use Changes and Elevated GHG Levels: The Case of Spring Precipitation in Tropical South America

Armineh Barkhordarian
University of California, Los Angeles

Hans von Storch
Helmholtz- Zentrum Geesthacht

Ali Behrangi
California Institute of Technology

Paul C. Loikith
Portland State University, ploikith@pdx.edu

Carlos R. Mechoso
University of California Los Angeles

Citation Details
Barkhordarian, A., von Storch, H., Behrangi, A., Loikith, P. C., Mechoso, C. R., & Detzer, J. (2018). Simultaneous Regional Detection of Land-Use Changes and Elevated GHG Levels: The Case of Spring Precipitation in Tropical South America. Geophysical Research Letters, 45, 6262–6271.

Geophysical Research Letters

RESEARCH LETTER
10.1029/2018GL078041

Key Points:
- The recently observed "drier dry season" over tropical South America is externally and systematically forced
- GHG and land-use change are attributed as key causes for the observed drying over the southern Amazonia and central Brazil over 1983–2012
- The recently observed "drier dry season" will continue and intensify in the course of unfolding anthropogenic climate change

Supporting Information:
- Supporting Information S1

Correspondence to:
A. Barkhordarian,
armineh.barkhordarian@jpl.nasa.gov

Citation:
Barkhordarian, A., von Storch, H., Behrangi, A., Loikith, P. C., Mechoso, C. R., & Detzer, J. (2018). Simultaneous regional detection of land-use changes and elevated GHG levels: The case of spring precipitation in tropical South America. *Geophysical Research Letters*, *45*, 6262–6271. https://doi.org/10.1029/2018GL078041

Received 30 MAR 2018
Accepted 1 JUN 2018
Accepted article online 8 JUN 2018
Published online 29 JUN 2018

Simultaneous Regional Detection of Land-Use Changes and Elevated GHG Levels: The Case of Spring Precipitation in Tropical South America

Armineh Barkhordarian[1,2], Hans von Storch[3], Ali Behrangi[2,4], Paul C. Loikith[5], Carlos R. Mechoso[1], and Judah Detzer[5]

[1]Department of Atmospheric and Oceanic Sciences, University of California, Los Angeles (UCLA), Los Angeles, CA, USA, [2]Jet Propulsion Laboratory, California Institute of Technology, Pasadena, CA, USA, [3]Institute of Coastal Research, Helmholtz-Zentrum Geesthacht, Geesthacht, Germany, [4]Department of Hydrology and Atmospheric Sciences, University of Arizona, Tucson, AZ, USA, [5]Department of Geography, Portland State University, Portland, OR, USA

Abstract A decline in dry season precipitation over tropical South America has a large impact on ecosystem health of the region. Results here indicate that the magnitude of negative trends in dry season precipitation in the past decades exceeds the estimated range of trends due to natural variability of the climate system defined in both the preindustrial climate and during the 850–1850 millennium. The observed drying is associated with an increase in vapor pressure deficit. The univariate detection analysis shows that greenhouse gas (GHG) forcing has a systematic influence in negative 30-year trends of precipitation ending in 1998 and later on. The bivariate attribution analysis demonstrates that forcing by elevated GHG levels and land-use change are attributed as key causes for the observed drying during 1983–2012 over the southern Amazonia and central Brazil. We further show that the effect of GS signal (GHG and sulfate aerosols) based on RCP4.5 scenario already has a detectable influence in the observed drying. Thus, we suggest that the recently observed "drier dry season" is a feature which will continue and intensify in the course of unfolding anthropogenic climate change. Such change could have profound societal and ecosystem impacts over the region.

Plain Language Summary This study uses statistical techniques to attribute the recently observed "drier dry season" over tropical South America to external drivers of climate change, both human-induced and naturally occurring. A decline in dry season precipitation has a large impact on ecosystem health of the region. Thus, attributing the forced components of the observed "drier dry season" to external drivers of climate change is of great practical importance to societies. Results indicate that the observed drying is well beyond the range of trends due to natural variability of the climate system and is found to be systematically and externally forced. The forcing by elevated greenhouse gas levels and land-use change (mainly deforestation) are attributed as key causes for the observed drying over the southern Amazonia and central Brazil. We further demonstrate that the recently observed "drier dry season" is a feature which will continue and intensify in the course of unfolding anthropogenic climate change. Such an assessment is critical for adaptation planning and mitigation strategies.

1. Introduction

The frequency and geographic patterns of rainfall are key climate features for many tropical countries around the world (Chadwick et al., 2016). Well-planned adaptation and mitigation strategies require knowledge on how these patterns would change in response to anthropogenic forcing (Sarojini et al., 2016). Bindoff et al. (2013) concludes that globally, an anthropogenic contribution to precipitation trends over land is likely since the 1950s. A decrease of the Northern Hemisphere precipitation during the 1950–1980 period and a subsequent recovery has been attributed to anthropogenic aerosols (Wu et al., 2013). Human-induced rainfall changes have also been detected over land in the northern middle to high latitudes (Min et al., 2008; Wan et al., 2014). To better assess the pace of precipitation change, we will need a better understanding of the influence of external forcing and natural variation (Stott et al., 2010). In tropical regions (30°S–30°N) the effect of external forcing has been detected in observed wet region precipitation during 1988–2014 (Polson & Hegerl, 2017) and in tropical precipitation satellite observations over 1988–2010 (Polson et al., 2013). Global climate models are projecting that seasonal precipitation response in the tropics to global warming

is a hybrid of wet-get-wetter and warmer-get-wetter effects (Huang et al., 2013; Seth et al., 2011). In contrast, sea surface temperature warming reduces continental precipitation in those regions that cannot meet the increasing demand for near-surface moist static energy (Chou & Neelin, 2004; Dwyer et al., 2014). In the Amazon rain forest the year 2010 featured a widespread drought (Lewis et al., 2011), which was even more severe than the "once-in-a-century" drought of 2005 (Marengo et al., 2008, 2011). Cox et al. (2008) suggested that 2005-like droughts would increase in Amazonia under conditions of increased greenhouse gases (GHGs). The recently observed warming in the dry seasons over tropical South America (SA) is well beyond the range of trends due to natural (internal) variability of the climate system (Barkhordarian et al., 2017). Besides the regional manifestation of GHG forcing, the indirect effect of black carbon aerosols on cloud cover has a detectable influence on the regional amplification of daytime warming in the dry seasons. However, in the wet season, recurrent natural modes of variability explain a substantial portion of temperature variability over SA (Barkhordarian et al., 2017).

At interannual time scale, dry season rainfall over SA is influenced by the increase in the tropical north south Atlantic sea surface temperature gradient and warmer eastern equatorial Pacific (Fu et al., 2001). The present study used statistical techniques to assess, for the first time, whether long-term (30-year) trends in dry season precipitation can be detected as being systematically (externally) forced and investigate to what extent observed changes can be attributed to external drivers of climate change, both human induced (well-mixed GHGs, anthropogenic aerosols, and land-use change, LU) and naturally occurring (solar irradiance and stratospheric aerosols due to volcanoes). A decline in dry season precipitation plays a critical role in hydroecosystem of the region (Cook et al., 2012; Saatchi et al., 2007). Thus, attributing the forced components of the observed "drier dry season" over tropical SA to external drivers of climate change is of great practical importance to societies.

In other words, our focus is on the following question: Are we observing systematic trends of rainfall or are we solely witnessing the effects of natural internal variability of the climate system? Such an assessment has not been done before for SA precipitation to our knowledge.

2. Data and Methodology

Our studied domain encompasses the tropical SA, defined here as the region from 85°W to 32°W and 25°S to 8°S. We have chosen this region because of the dominance of convective processes and the concurrent regional emergence of the dry and wet seasons. We investigate precipitation changes in August-September-October (ASO), which corresponds to dry and transitional months. The observational record for precipitation is obtained from the monthly Global Precipitation Climatology Centre (GPCC) full v.7 data set for the years 1901–2013 (Schneider et al., 2011) and the monthly satellite-based Global Precipitation Climatology Project (GPCP) gridded data set (version 2.3; Adler et al., 2017) for the years 1979–2016. The latter data set uses Special Sensor Microwave/Imager measurements, which results in more reliable trends (Hegerl et al., 2015). Historical and future climate projections are based on the Coupled Model Intercomparison Project Phase 5 (CMIP5) archive (see Table S1 in the supporting information; Taylor et al., 2012). In order to address finer scale features of climate change signals, we also use REMO2009 regional climate model driven by MPI-ESM-LR from WCRP CORDEX (Jones et al., 2011). For estimation of natural (internal) variability, we employ the 12,000-yearlong preindustrial control simulations derived from CMIP5 archive. We further use the fourth version of the Community Climate System Model's (CCSM4) Millennium simulations over 0850–1850 (Gent et al., 2011) to obtain an estimate of natural (internal + external) variability.

We follow the same methodology used in Barkhordarian et al. (2013, 2016, 2017). Our first step consists of assessing whether systematically (externally) forced changes are detectable in the observed precipitation change. This is achieved by testing the null hypothesis that the observed change is drawn from the population of an undisturbed climate. In the second step, we examine the null hypothesis that the observed change is drawn from a hypothetical population of a climate disturbed by a specific external influence. The determination of the hypothetical population of a climate disturbed with changes in aerosol loads, GHGs, or LU are derived from simulations of the response to such forcings. The patterns, which such simulations suggest, are named "guess patterns" (Hasselmann, 1993). We project the observed changes on these guess patterns by using univariate and bivariate regression analysis. This provides a plausibility argument that the driver behind the guess pattern could be the cause for the observed change. We note that this is not a reason to claim that

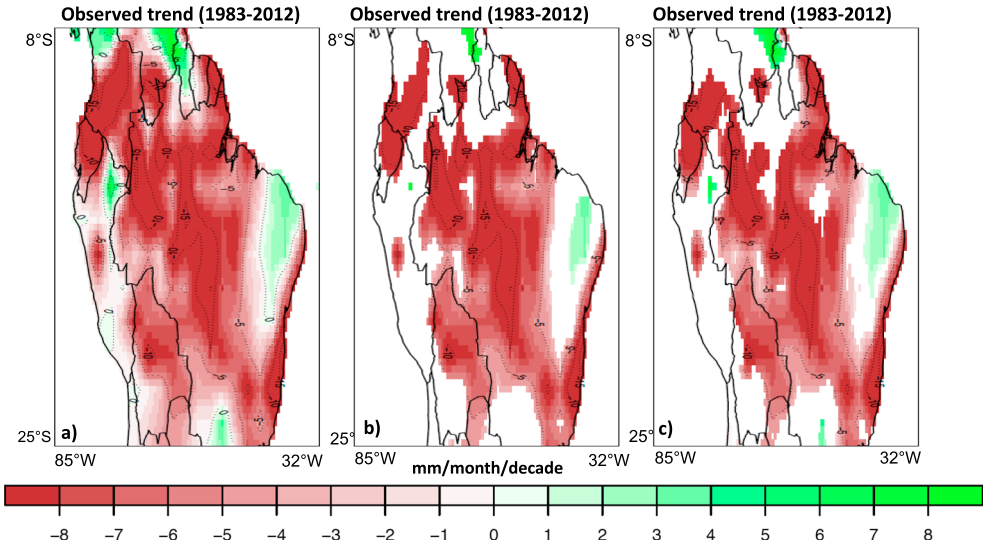

Figure 1. (a) Observed precipitation trends in August-October over the 1983–2012 time period based on Global Precipitation Climatology Project data set. (b) Regions where externally forced changes are detectable (at 5% level) in the observed record, based on preindustrial control simulations. (c) Regions where externally forced changes are detectable (at 5% level) in the observed record, based on millennium simulations of CCSM4 model (0850–1850).

the detected signal is the sole or even the dominant forcing. This is in particular so, when the guess patterns of two different forcings share a markedly spatial similarity. In this case a simultaneous attribution analysis is required (bivariate regression).

To estimate climate change signals, we use two approaches. The first approach uses the output from transient historical simulations in the CMIP5 archive. These are organized in four groups, according to where the forcing includes just a single component, which is either (1) well-mixed GHGs; (2) natural external forcing, including solar forcing and stratospheric aerosols due to volcanoes (NAT); (3) anthropogenic aerosols (AAs); or (4) LU. More details on the simulations in these groups are given in Text S1 in the supporting information. The second approach uses time-slice climate change experiment to define GS signal (GHG and sulfate aerosols) based on RCP4.5 scenario (see Text S1; Bhend & von Storch, 2009). The strategy is giving each model equal weight when computing multimodel ensemble mean (Allen & Tett, 1999). In total, we have 24 GS response patterns derived from 23 GCMs from the CMIP5 archive and 1 RCM from CORDEX.

3. Results

3.1. Detection of Systematically Forced Changes in Precipitation

Figure 1a shows the 30-year trend of observed precipitation in ASO for the period 1983–2012 based on the GPCP data set (for GPCC data set see Figure S1 in the supporting information). Both GPCP and GPCC data sets agree on a general precipitation decreases over tropical SA, except for local increases over Northeast Brazil. A general drying in northern Amazonia since the 1970s has also been reported (e.g., Marengo, 2004). Here we cinvestigate whether systematically forced changes have a detectable influence on the observed record of precipitation. This is achieved by testing the null hypotheses that the observed trends are within the 5–95th percentile distribution of unforced trends derived from preindustrial control simulations. Because models tend to underestimate observed variability in precipitation, particularly in the tropics (Polson et al., 2013; Zhang et al., 2007), the model variance is doubled in calculation of the internal variability range (Polson & Hegerl, 2017). The results are shown in Figure 1b, which shows areas where the observed trends are larger than what could be just due to natural (internal) variability. Externally forced changes are detectable on the decreasing precipitation trend observed over Brazil, northern Bolivia, southern Colombia, and Ecuador (with less than 5% risk of error). However, the observed drying trends over Peru, southern Bolivia, and wetting trends over Northeast Brazil are within the range due to natural (internal) variability of the climate system.

These results remain robust against comparing the observed trends with the distribution of naturally forced trends derived from millennium simulations of CCSM4 model (0850–1850; Figure 1c). The similarity between Figures 1b and 1c suggests a negligible influence of natural external forcing (variation in Solar forcing and stratospheric aerosols due to volcanoes) in the observed drying over the region. The detection results presented in the next section using natural-forcing-only simulations (NAT) confirm this statement. However, at centennial time scale, solar forcing appears to be one the drivers effecting South American monsoon system intensity (Novello et al., 2017).

3.2. Univariate Signal Detection

The drying over tropical SA is observed and also simulated in GHG-forcing only simulations (Figure S2a). In addition, both GCMs (Figure S3, CMIP5) and RCM (Figure S2c, CORDEX) show widespread drying over tropical SA in response to GS forcing, suggesting agreement among CORDEX RCM-based and CMIP5 GCM-based projections. These are also consistent features in the previous generation scenarios (A1B, A2; IPCC Climate Change, 2013; Vera et al., 2006). The LU forcing-only simulations suggest a decrease in precipitation over Brazil, with areas of increasing precipitation over northern Amazonia (Figure S2b). Dry season rainfall is more often associated with locally generated convection and is more sensitive to LU (Malhi et al., 2008). In the tropics, the net impact of deforestation is typically a nonradiative warming due primarily to decreasing evapotranspiration and surface roughness (Jackson et al., 2008; Sanderson et al., 2012), which is a decrease in latent heat flux (larger sensible heating), along with a decrease in precipitation (Lawrence & Vandecar, 2015; Pielke et al., 2002). Based on climate model simulations, deforestation in 2010 decreases the annual mean rainfall across the Amazon basin by 1.8 ± 0.3% (Spracklen & Garcia-Carreras, 2015). Roy and Avissar (2002) also demonstrate that large-scale LU tends to reduce rainfall.

Here we examine the null hypothesis that the observed change in precipitation is drawn from a hypothetical population of a climate disturbed by a specific external influence. With this purpose, we project the observed changes on the guess patterns of GS, GHG, LU, AA, and NAT forcing. Figure 2 (top) displays the scaling factors of observed precipitation changes over tropical SA in ASO against 23 GS guess patterns derived from CMIP5 based on the RCP4.5 scenario (black bars), together with those against GHG guess pattern, the NAT guess pattern, the AA guess pattern, the LU guess pattern, and the GS guess pattern derived from CORDEX. The whiskers indicate the 95th percentile uncertainty range of scaling factors in a stationary climate based on 400 control run segments, for the raw and double the model variance. Because rainfall over tropical SA is underestimated in some of the CMIP5 models (Yin et al., 2013), the model variance is doubled in calculation of the internal variability range.

According to Figure 2 (top), the uncertainty range of scaling factors does not include zero line, in 19 out of 23 GS guess patterns derived from CMIP5 (black bars), the GS derived from CORDEX (red bar), and the GHG (blue bar). Therefore, we conclude that GS and GHG forced signals are detectable in the observed precipitation decrease in the 1983–2012 time period. In addition, we can see that the LU forced signal is also detectable at the 5% significant level. The region in which externally forced changes are detectable over 1983–2012 encompasses the Amazon rainforest. More than 20% of the Amazon rainforest has been cleared in the past three decades (Khanna et al., 2017). Thus, detection of LU signal is plausible in the region. The AA-only forcing simulations (purple bar) display negative scaling factor, indicating a response that is opposite to the observations. Natural-forcing-only simulations (yellow bar) show near zero scaling factor, indicating negligible influence of natural external forcing (variation in Solar forcing and stratospheric aerosols due to volcanoes) in the observed drying over the region.

Figure 2 (bottom) shows locations over the southern Amazonia and central Brazil where the effect of GHG, LU, and GS signals are detectable (at 5% level). The claim that we "detect the LU-signal" means that a projection on the pattern derived from the LU scenarios leads to two conclusions: (a) The observed signal contradicts the null hypothesis of "no external forcing," and (b) the observed signal is not contradicting the null-hypothesis of "a response to LU." This does not mean that LU is really the cause—this is in particular so, when the GHG guess pattern is similar to the LU guess pattern (see Figures S2a and S2b). In this case a simultaneous (bivariate) attribution analysis is required. In the next section we examine the attribution of the observed signal to the two possible contributors, GHG and LU, by using two-dimensional (bivariate) regression analysis.

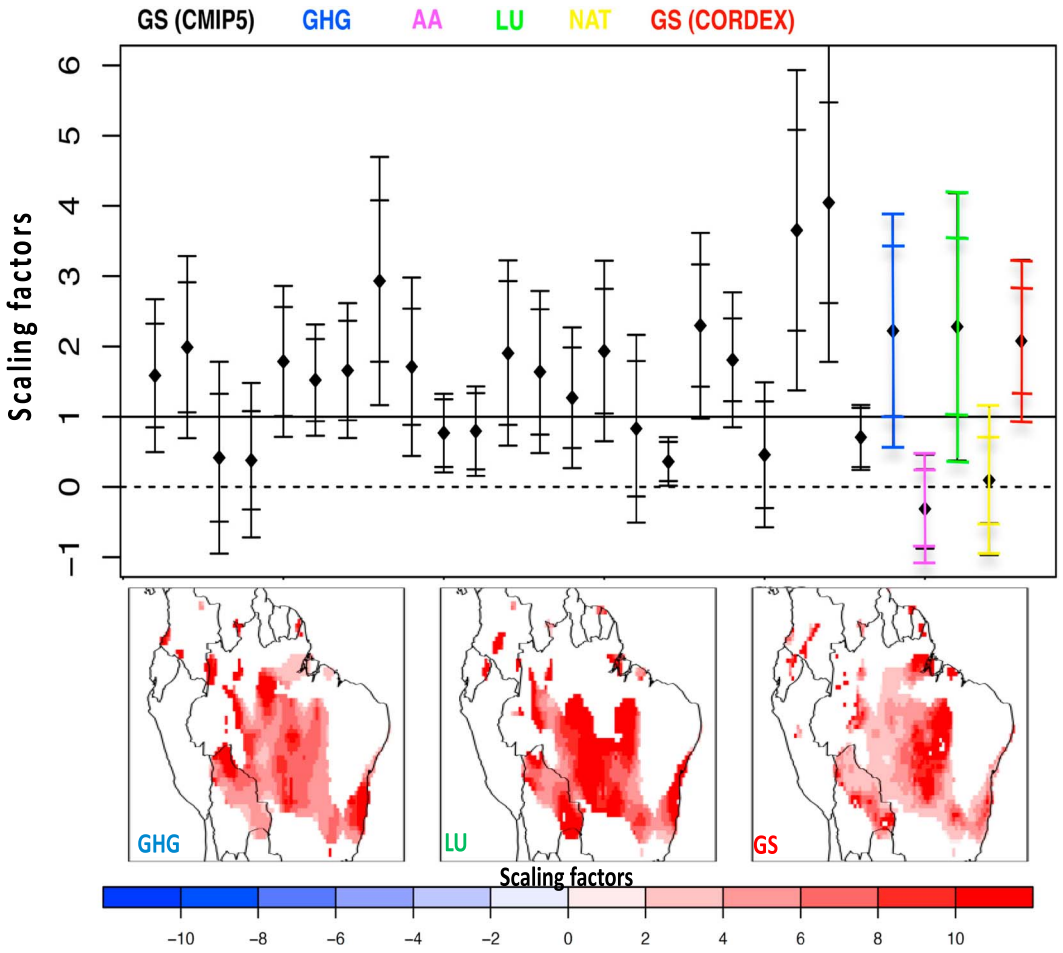

Figure 2. (top) Scaling factors of observed precipitation changes over tropical South America in August-October against 23 greenhouse gas (GHG) and sulfate aerosol signal guess patterns (Coupled Model Intercomparison Project Phase 5) based on the RCP4.5 scenario (black bars), against the simulated GHG signal (blue bars), the anthropogenic aerosol signal (purple bar), the land-use change signal (green bar), the natural external forcing signal (yellow bar), and the GHG and sulfate aerosol signal derived from CORDEX (red bar). The whiskers show the 95th percentile range of uncertainties associated with scaling factors for the raw and double the model variance, derived from 12,000-year control simulations. Detection of a climate change signal can be claimed in those cases where the whiskers do not include the zero line. (bottom) Regions where scaling factors are significantly greater than zero compared with natural variations, indicating locations where the effect of climate change signals is detectable in observed precipitation record (at 5% level).

3.3. Bivariate Signal Attribution

In order to consider the combined influence of GHG and LU signals, we carry out a two-dimensional attribution analysis when observed data are projected onto two guess patterns of GHG (Figure S2a) and LU (Figure S2b) simultaneously during 1983–2012 time period. The attribution of two hypothetical signals is shown in Figure 3a. When we do the attribution part separately for the two suspected drivers, GHG and LU, we get an intervals of the univariately estimated scaling factors (blue whiskers), which are added into the diagram of the bivariate ellipse of the simultaneous attribution analysis. The one-dimensional uncertainty intervals for the univariate and bivariate analysis for two signals are shown as blue and black whiskers, respectively. GHG is detected since the horizontal whiskers lies to the right of *y* axes and LU is detected since the vertical whiskers lies above the *x* axes. The two-dimensional (bivariate) uncertainty contour for the GHG and LU is shown with an ellipse. The ellipse containing 90% of the estimated joint distribution of scaling factors for two signals excludes the origin (0,0), indicating that the effects of GHG and LU signals are detectable simultaneously. In addition, the scaling factors are consistent with unit amplitude since the point (1,1) lies

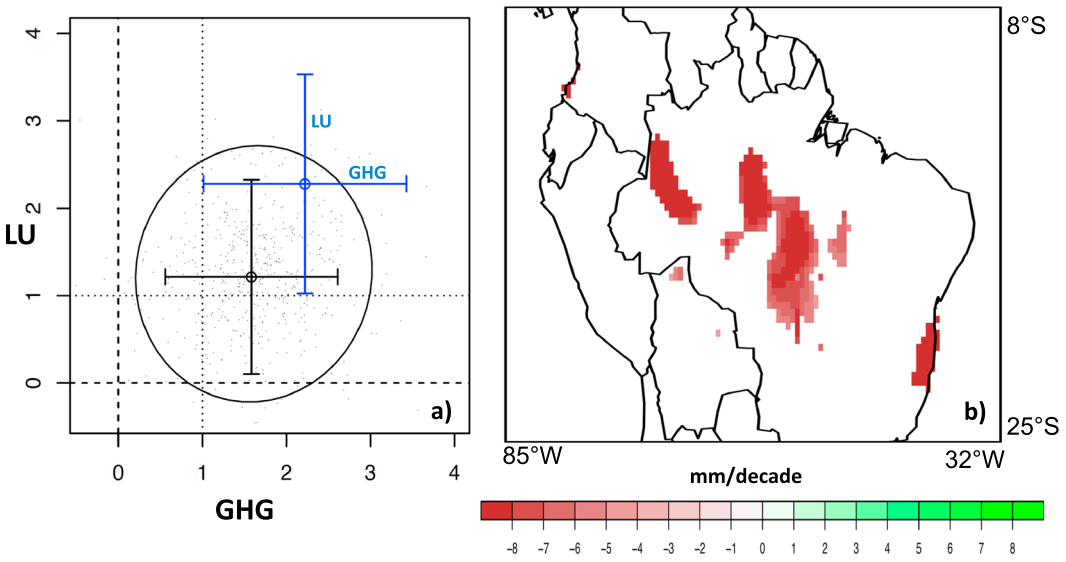

Figure 3. (a) The ellipse displays the joint two-dimensional 90% uncertainty interval for the greenhouse gas (GHG) and land-use change (LU) when observed data are regressed onto two signals simultaneously during 1983–2012. The black and blue whiskers indicate the bivariate and univariate one-dimensional 95th percentile uncertainty intervals for the two signals, respectively. (b) Regions where externally forced changes are still detectable after removing the effect of GHG and LU forcing (at 5% level).

within the ellipse. Thus, we conclude here simultaneous regional detection and attribution of LU and GHG forced signals over tropical SA.

In order to decide if our attribution study is complete, we derive the unexplained part in local scale. We subtract the attributed changes from the observed change and examine if we detect a remaining external forcing. We do it univariately, that is, for all grid points separately. We examine if the remaining trends are larger than could be expected from natural variations (as provided by the control simulations). Figure 3b shows small regions mainly located over Amazon basin, of the order of ~8% of all grid points, where systematically forced changes are still detectable in the remaining trend after removing the effect of GHG and LU. We note here that we adopt a risk of false rejection ($<$5%) of the null hypothesis of "no external forcing." As suggested by von Storch (1982) when the regional null hypothesis is valid, on an average $n = 0.05$ m (m number of grid points), local alternatives will falsely be rejected.

3.4. Assessing the Drivers in Linear Trends of Precipitation Over Time

Here we analyze the drivers in linear trends of precipitation over time. The GPCC data set suggests an early period (in 1980s) with increasing precipitation over Tropical SA (Figure S4). The significant positive trends observed in 1980s, which is beyond the 90th percentile range of natural (internal) variability, could be due to effects of small-scale deforestation (a few kilometers in extent) in the 1980s over Amazon. This has caused thermally triggered atmospheric circulations (Roy & Avissar, 2002) that contributed to enhance regional cloudiness (Wang et al., 2009) and rainfall (Chagnon & Bras, 2005). However, the rate of change toward wetter conditions decreases with time and again exceeds the limits of natural variability for 30-year trends ending in 1997 and later on (Figure S4). The strongest drying is during 1972–2003 with about −18 mm/month decrease in the amount of precipitation over tropical SA.

The 1-year moving scaling factors of precipitation over the period 1952–2012 in GPCC (1979–2016 in GPCP), onto the guess patterns of GS, GHG, NAT, AA, and LU, are displayed in Figures 4a–4e, respectively. The gray shaded area indicates the 95th percentile uncertainty range based on 400 control run segments, for the raw and double the model variance. Detection of a climate change signal can be claimed in those cases where the gray shaded area excludes "0." We find that the GS signal derived from CORDEX (Figure 4a) and also the GHG signal derived from CMIP5 (Figure 4b) have a constant and systematic influence in the observed 30-year

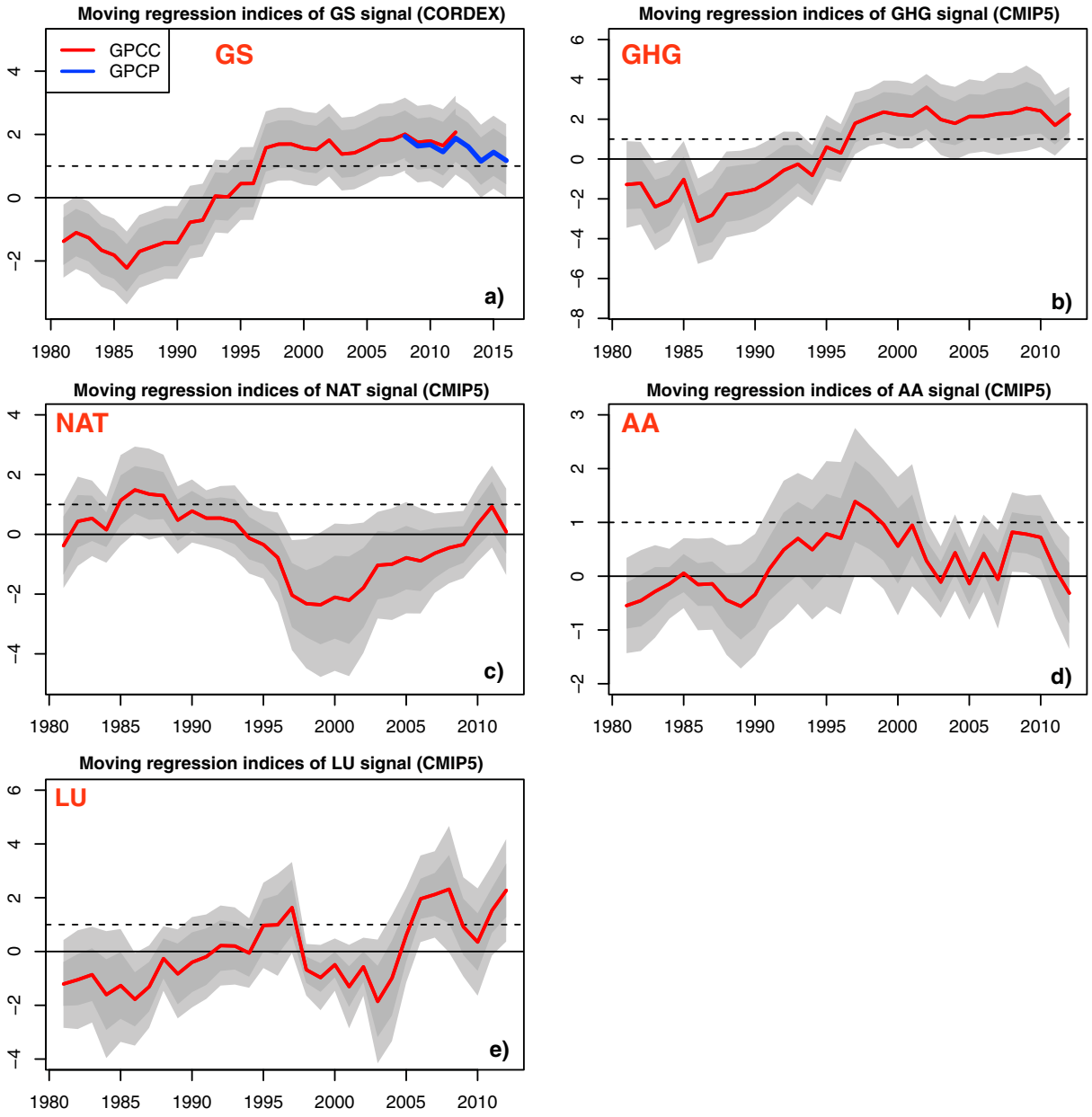

Figure 4. (a) Scaling factors of observed 1-year moving 30-year trends of precipitation in August-October based on Global Precipitation Climatology Centre (red curves) and Global Precipitation Climatology Project (blue curves) onto the greenhouse gas (GHG) and sulfate aerosol signal guess pattern (CORDEX and RCP4.5), (b) scaling factors of observed trends onto the historical multimodel mean GHG guess pattern, (c) the natural external forcing guess pattern (NAT), (d) the anthropogenic aerosol guess pattern (AA), and (e) the land-use change guess pattern (LU). *The horizontal axes* show the end-year of moving 30-year trends. The *gray shaded* area indicates the 95th percentile range in a stationary climate based on 400 control run segments, for the raw and double the model variance. Detection of a signal can be claimed in those cases where the gray shaded area excludes "0."

trends of precipitation ending in 1998 and later on (with less than 5% risk of error, one-sided test). The scaling factors of the NAT and AA signals are, with a few exceptions, never significantly different from zero.

4. Discussions and Conclusions

It is shown here that the recently observed "drier dry season" is a feature which is externally and systematically forced (<5% risk of error). Results are robust against doubling the model variance when estimating internal variability. The univariate detection analysis shows that GHG forcing has a constant and systematic

influence in negative 30-year trends of precipitation ending 1998 and later on. The bivariate attribution analysis demonstrates that forcing by elevated GHG levels and LU are attributed (<5% risk of error) as key causes for the observed drying during 1983–2012 over the southern Amazonia and central Brazil.

At the local scale, after removing the effect of GHG and LU, externally forced changes are still detectable in the residual trend over center of Brazil. This indicates that either climate models underestimate the response to the forcing at local scale or other external drivers and/or local feedbacks are at work. Given that over the residual areas, shown in Figure 3b, continental evapotranspiration provides the main moisture source for precipitation, vapor pressure deficit (VPD) feedback could be a likely candidate as high VPD can inhibit precipitation formation (Behrangi et al., 2016; Seager et al., 2015). The recently observed positive trend in incoming solar radiation reaching the surface of northern SA in the dry season could partly be attributed to cloud reduction due to radiatively absorbing aerosols such as black carbon (Barkhordarian et al., 2017). This produces a daytime warming amplification over tropical SA. Thus, as the climate continues to warm over the region, further drying over land is expected (Trenberth et al., 2013). This results in two mechanisms: greater change in potential evapotranspiration over land compared to the ocean (Sherwood & Fu, 2014) and land-atmosphere feedbacks that amplify aridity increase over land (Berg et al., 2016). This drying will lead to growing differences between actual and saturation water vapor concentrations, defined as the VPD, and reduction of relative humidity. The ERA-Interim reanalysis data (Dee et al., 2011) shows an increasing trend of VPD on the order of +0.2 (KPa/decade) in ASO over 1983–2012, which is more pronounced over Brazil (Figure S5). The observed increasing VPD (Figure S5) under climatic warming that causes higher atmospheric demand for water could also reduce forest CO_2 uptake (Brzostek et al., 2014; Sulman et al., 2016), representing a positive climate change feedback (Trenberth et al., 2013).

Taking the ensemble of 24 CMIP5 and CORDEX models as a crude metric of probabilities, we further show that with 20 out of 24 models analyzed, the effect of GS signal (GHG and AAs) based on RCP4.5 scenario already has a detectable influence in the observed drying over the region (at 5% significant level). Thus, we suggest that the observed "drier dry season" over southern Amazonia and central Brazil is a feature which will continue and intensify in the course of unfolding anthropogenic climate change. Such an assessment is critical for adaptation planning and mitigation strategies.

Acknowledgments
We acknowledge the support provided by the National Science Foundation AGS-1547899. The CMIP5 and CORDEX data were obtained from LLNL node of the Earth System Grid Federation (ESGF). GPCC and GPCP precipitation data are provided at climatedataguide.ucar.edu and www.ncdc.noaa.gov, respectively. CCSM4 data are provided at www.earthsystemgrid.org.

References

Adler, R. F., Gu, G., Sapiano, M., Wang, J.-J., & Huffman, G. J. (2017). Global precipitation: Means, variations and trends during the satellite era (1979–2014). *Surveys in Geophysics*, *38*(4), 679–699. https://doi.org/10.1007/s10712-017-9416-4

Allen, M. R., & Tett, S. F. B. (1999). Checking for model consistency in optimal fingerprinting. *Climate Dynamics*, *15*(6), 419–434. https://doi.org/10.1007/s003820050291

Barkhordarian, A., von Storch, H., & Bhend, J. (2013). The expectation of future precipitation change over the Mediterranean region is different from what we observe. *Climate Dynamics*, *40*(1-2), 225–244. https://doi.org/10.1007/s00382-012-1497-7

Barkhordarian, A., von Storch, H., Zorita, E., & Gómez-Navarro, J. (2016). An attempt to deconstruct recent climate change over the Baltic Sea basin. *Journal of Geophysical Research: Atmosphere*, *121*, 13,207–13,217. https://doi.org/10.1002/2015JD024648

Barkhordarian, A., von Storch, H., Zorita, E., Loikith, P. C., & Mechoso, C. R. (2017). Observed warming over northern South America has an anthropogenic origin. *Climate Dynamics*. https://doi.org/10.1007/s00382-017-3988-z

Behrangi, A., Fetzer, E. J., & Granger, S. L. (2016). Early detection of drought onset using near surface temperature and humidity observed from space. *International Journal of Remote Sensing*, *37*(16), 3911–3923. https://doi.org/10.1080/01431161.2016.1204478

Berg, A., Findell, K., Lintner, B., Giannini, A., Seneviratne, S. I., van den Hurk, B., et al. (2016). Land-atmosphere feedbacks amplify aridity increase over land under global warming. *Nature Climate Change*, *6*(9), 869–874. https://doi.org/10.1038/nclimate3029

Bhend, J., & von Storch, H. (2009). Consistency of observed winter precipitation trends in northern Europe with regional climate change projections. *Climate Dynamics*, *31*, 17–28.

Bindoff, N. L., Stott, P. A., AchutaRao, K. M., Allen, M. R., Gillett, N., Gutzler, D., et al. (2013). Detection and attribution of climate change: From global to regional. In T. F. Stocker, et al. (Eds.), *Climate change 2013: The physical science basis* (pp. 867–952). UK and New York: Cambridge University Press.

Brzostek, E. R., Dragoni, D., Schmid, H. P., Rahman, A. F., Sims, D., Wayson, C. A., et al. (2014). Chronic water stress reduces tree growth and the carbon sink of deciduous hardwood forests. *Global Change Biology*, *20*(8), 2531–2539. https://doi.org/10.1111/gcb.12528

Chadwick, R., Good, P., Martin, G., & Rowell, D. P. (2016). Large rainfall changes consistently projected over substantial areas of tropical land. *Nature Climate Change*, *6*(2), 177–181. https://doi.org/10.1038/nclimate2805

Chagnon, F. J. F., & Bras, R. L. (2005). Contemporary climate change in the Amazon. *Geophysical Research Letters*, *32*, L13703. https://doi.org/10.1029/2005GL022722

Chou, C., & Neelin, J. D. (2004). Mechanisms of global warming impacts on regional tropical precipitation. *Journal of Climate*, *17*(13), 2688–2701. https://doi.org/10.1175/1520-0442(2004)017%3C2688:MOGWIO%3E2.0.CO;2

Cook, B., Zeng, N., & Yoon, J. (2012). Will Amazonia dry out? Magnitude and causes of change from IPCC climate model projections. *Earth Interactions*, *16*(3), 1–27. https://doi.org/10.1175/2011EI398.1

Cox, P. M., Harris, P. P., Huntingford, C., Betts, R. A., Collins, M., Jones, C. D., et al. (2008). Increasing risk of Amazonian drought due to decreasing aerosol pollution. *Nature*, *453*(7192), 212–215. https://doi.org/10.1038/nature06960

Dee, D. P., Uppala, S. M., Simmons, A. J., Berrisford, P., Poli, P., Kobayashi, S., et al. (2011). The ERA-Interim reanalysis: Configuration and performance of the data assimilation system. *Quarterly Journal of the Royal Meteorological Society*, *137*(656), 553–597. https://doi.org/10.1002/qj.828

Dwyer, J. G., Biasutti, M., & Sobel, A. H. (2014). The effect of greenhouse gas-induced changes in SST on the annual cycle of zonal mean tropical precipitation. *Journal of Climate*, *27*(12), 4544–4565. https://doi.org/10.1175/JCLI-D-13-00216.1

Fu, R., Dickinson, R. E., Chen, M., & Wang, H. (2001). How do tropical sea surface temperatures influence the seasonal distribution of precipitation in the equatorial Amazon? *Journal of Climate*, *14*(20), 4003–4026. https://doi.org/10.1175/1520-0442(2001)014%3C4003:HDTSST%3E2.0.CO;2

Gent, P. R., Danabasoglu, G., Donner, L. J., Holland, M. M., Hunke, E. C., Jayne, S. R., et al. (2011). The Community Climate System Model version 4. *Journal of Climate*, *24*(19), 4973–4991. https://doi.org/10.1175/2011JCLI4083.1

Hasselmann, K. (1993). Optimal fingerprints for the detection of time-dependent climate change. *Journal of Climate*, *6*(10), 1957–1971. https://doi.org/10.1175/1520-0442(1993)006%3C1957:OFFTDO%3E2.0.CO;2

Hegerl, G. C., Black, E., Allan, R. P., Ingram, W. J., Polson, D., Trenberth, K. E., et al. (2015). Challenges in quantifying changes in the global water cycle. *Bulletin of the American Meteorological Society*, *96*(7), 1097–1115. https://doi.org/10.1175/BAMS-D-13-00212.1

Huang, P., Xie, S. P., Hu, K., Huang, G., & Huang, R. (2013). Patterns of the seasonal response of tropical rainfall to global warming. *Nature Geoscience*, *6*(5), 357–361. https://doi.org/10.1038/ngeo1792

IPCC Climate Change (2013). In T. F. Stocker, et al. (Eds.), *The physical science basis*. Cambridge, UK, and New York: Cambridge University Press.

Jackson, R. B., Randerson, J. T., Canadell, J. G., Anderson, R. G., Avissar, R., Baldocchi, D. D., et al. (2008). Protecting climate with forests. *Environmental Research Letters*, *3*(4), 044006.

Jones, C., Giorgi, F., & Asrar, G. (2011). The Coordinated Regional Downscaling Experiment: CORDEX, An international downscaling link to CMIP5: CLIVAR Exchanges (No. 56, Vol. 16, pa. 34–40).

Khanna, L., Medvigy, D., Fueglistaler, S., & Walko, R. (2017). Regional dry-season climate changes due to three decades of Amazonian deforestation. *Nature Climate Change*, *7*(3), 200–204. https://doi.org/10.1038/nclimate3226

Lawrence, D., & Vandecar, K. (2015). Effects of tropical deforestation on climate and agriculture. *Nature Climate Change*, *5*(1), 27–36. https://doi.org/10.1038/nclimate2430

Lewis, S. L., Brando, P. M., Phillips, O. L., van der Heijden, G. M. F., & Nepstad, D. (2011). The 2010 Amazon drought. *Science*, *331*(6017), 554. https://doi.org/10.1126/science.1200807

Malhi, Y., Timmons Roberts, J., Betts, R. A., Killeen, T. J., Li, W., & Nobre, C. A. (2008). Climate change, deforestation, and the fate of the Amazon. *Science*, *319*(5860), 169–172. https://doi.org/10.1126/science.1146961

Marengo, J. A. (2004). Interdecadal variability and trends of rainfall across the Amazon basin. *Theoretical and Applied Climatology*, *78*, 79–96.

Marengo, J. A., Nobre, C. A., Tomasella, J., Oyama, M. D., Oliveira, G. S., de Oliveira, R., et al. (2008). The drought of Amazonia in 2005. *Journal of Climate*, *21*(3), 495–516. https://doi.org/10.1175/2007JCLI1600.1

Marengo, J. A., Tomasella, J., Alves, L. M., Soares, W. R., & Rodriguez, D. A. (2011). The drought of 2010 in the context of historical droughts in the Amazon region. *Geophysical Research Letters*, *38*, L12703. https://doi.org/10.1029/2011GL047436

Min, S., Zhang, X., & Zwiers, F. W. (2008). Human-induced Arctic moistening. *Science*, *320*(5875), 518–520. https://doi.org/10.1126/science.1153468

Novello, V. F., Cruz, F. W., Vuille, M., Stríkis, N. M., Edwards, R. L., Cheng, H., et al. (2017). A high-resolution history of the south American monsoon from Last Glacial Maximum to the Holocene. *Scientific Reports*, *7*, 44267. https://doi.org/10.1038/srep44267

Pielke, R. A., Marland, G., Betts, R. A., Chase, T. N., Eastman, J. L., Niles, J. O., & Running, S. W. (2002). The influence of land use change and landscape dynamics on the climate system: Relevance to climate-change policy beyond the radiative effect of greenhouse gases. *Philosophical Transactions of the Royal Society A*, *360*(1797), 1705–1719. https://doi.org/10.1098/rsta.2002.1027

Polson, D., & Hegerl, G. (2017). Strengthening contrast between precipitation in tropical wet and dry regions. *Geophysical Research Letters*, *44*, 365–373. https://doi.org/10.1002/2016GL071194

Polson, D., Hegerl, G. C., Zhang, X., & Osborn, T. J. (2013). Causes of robust seasonal land precipitation changes. *Journal of Climate*, *26*(17), 6679–6697. https://doi.org/10.1175/JCLI-D-12-00474.1

Roy, S. B., & Avissar, R. (2002). Impact of land use/land cover change on regional hydrometeorology in Amazonia. *Journal of Geophysical Research*, *107*(D20), 8037. https://doi.org/10.1029/2000JD00026

Saatchi, S. S., Houghton, R. A., Soares, J. V., & Yu, Y. (2007). Distribution of aboveground live biomass in the Amazon basin. *Global Change Biology*, *13*(4), 816–837. https://doi.org/10.1111/j.1365-2486.2007.01323.x

Sanderson, M., Pope, E., Santini, M., Mercogliano, P., & Montesarchio, M. (2012). Influences of EU forests on weather patterns: Final report. Report for the European commission (DG-Environment). Retrieved from http://ec.europa.eu/environment/forests/pdf/EU_Forests_Final_Report.pdf

Sarojini, B. B., Stott, P. A., & Black, E. (2016). Detection and attribution of human influence on regional precipitation. *Nature Climate Change*, *6*(7), 669–675. https://doi.org/10.1038/nclimate2976

Schneider, U., Becker, A., Finger, P., Meyer-Christoffer, A., Rudolf, B., & Ziese, M. (2011). GPCC full data reanalysis version 6.0 at 0.5°: Monthly land-surface precipitation from rain-gauges built on GTS-based and historic data. https://doi.org/10.5676/DWD_GPCC/FD_M_V6_050

Seager, R., Hooks, A., Williams, A. P., Cook, B., Nakamura, J., & Henderson, N. C. (2015). Variability, and trends in the U.S. vapor pressure deficit, an important fire-related meteorological quantity. *Journal of Applied Meteorology and Climatology*, *54*(6), 1121–1141. https://doi.org/10.1175/JAMC-D-14-0321.1

Seth, A., Rauscher, S. A., Rojas, M., Giannini, A., & Camargo, S. J. (2011). Enhanced spring convective barrier for monsoons in a warmer world? *Climatic Change*, *104*(2), 403–414. https://doi.org/10.1007/s10584-010-9973-8

Sherwood, S., & Fu, Q. (2014). A drier future? *Science*, *343*(6172), 737–739. https://doi.org/10.1126/science.1247620

Spracklen, D. V., & Garcia-Carreras, L. (2015). The impact of Amazonian deforestation on Amazon basin rainfall. *Geophysical Research Letters*, *42*, 9546–9552. https://doi.org/10.1002/2015GL066063

Stott, P. A., Gillett, N. P., Hegerl, G. C., Karoly, D. J., Stone, D. A., Zhang, X., & Zwiers, F. (2010). Detection and attribution of climate change: A regional perspective. *WIREs Climate Change*, *1*(2), 192–211. https://doi.org/10.1002/wcc.34

Sulman, B. N., Roman, D. T., Yi, K., Wang, L., Phillips, R. P., & Novick, K. A. (2016). High atmospheric demand for water can limit forest carbon uptake and transpiration as severely as dry soil. *Geophysical Research Letters*, *43*, 9686–9695. https://doi.org/10.1002/2016GL069416

Taylor, K. E., Stouffer, R. J., & Meehl, G. A. (2012). An overview of Cmip5 and the experiment design. *Bulletin of the American Meteorological Society*, *93*(4), 485–498. https://doi.org/10.1175/Bams-D-11-00094.1

Trenberth, K. E., Dai, A., van der Schrier, G., Jones, P. D., Barichivich, J., Briffa, K. R., & Sheffield, J. (2013). Global warming and changes in drought. *Nature Climate Change*, *4*(1), 17–22. https://doi.org/10.1038/nclimate2067

Vera, C., Silvestri, G., Liebmann, B., & González, P. (2006). Climate change scenarios for seasonal precipitation in South America from IPCC-AR4 models. *Geophysical Research Letters*, *33*, L13707. https://doi.org/10.1029/2006GL025759

von Storch, H. (1982). A remark of Chervin/Schneider's algorithm to test significance of climate experiments with GCMs. *Journal of the Atmospheric Sciences*, *39*(1), 187–189. https://doi.org/10.1175/1520-0469(1982)039%3C0187:AROCSA%3E2.0.CO;2

Wan, H., Zhang, X., Zwiers, F., & Min, S.-K. (2014). Attributing northern high-latitude precipitation change over the period 1966–2005 to human influence. *Climate Dynamics*, *45*, 1713–1726.

Wang, J. F., Chagnon, F. J. F., Williams, E. R., Betts, A. K., Renno, N. O., Machado, L. A. T., et al. (2009). Impact of deforestation in the Amazon basin on cloud climatology. *Proceedings of the National Academy of Sciences of the United States of America*, *106*(10), 3670–3674. https://doi.org/10.1073/pnas.0810156106

Wu, P., Christidis, N., & Stott, P. A. (2013). Anthropogenic impact on Earth's hydrological cycle. *Nature Climate Change*, *3*(9), 807–810. https://doi.org/10.1038/nclimate1932

Yin, L., Fu, R., Shevliakova, E., & Dickinson, R. E. (2013). How well can CMIP5 simulate precipitation and its controlling processes over tropical South America? *Climate Dynamics*, *41*(11–12), 3127–3143. https://doi.org/10.1007/s00382-012-1582-y

Zhang, X., Zwiers, F., Hegerl, G., Lambert, F., Gillett, N., Solomon, S., et al. (2007). Detection of human influence on twentieth-century precipitation trends. *Nature*, *448*(7152), 461–465. https://doi.org/10.1038/nature06025